Article

Study on Accuracy Evaluation of MODIS AOD Products and Spatio-Temporal Distribution Characteristics of AOD in Hangzhou

Xiaohong Yuan [1,2], Yuji Xia [1], Jinqi He [1], Mengjia Cheng [1], Bing Qi [3], Zhifeng Yu [1,2,*] and Ben Wang [1,*]

[1] Institute of Remote Sensing and Earth Sciences, School of Information Science and Engineering, Hangzhou Normal University, Hangzhou 311121, China; yuanxh@hznu.edu.cn (X.Y.); 2021213101027@stu.hznu.edu.cn (Y.X.); 2021213101013@stu.hznu.edu.cn (J.H.); 2017210214030@stu.hznu.edu.cn (M.C.)

[2] Zhejiang Provincial Key Laboratory of Urban Wetlands and Regional Change, Hangzhou 311121, China

[3] Hangzhou Meteorological Bureau, Hangzhou 310051, China; bill_129@sina.com

[*] Correspondence: yu@hznu.edu.cn (Z.Y.); 20170056@hznu.edu.cn (B.W.)

Abstract: In recent years, although the quality of the atmospheric environment has improved in some regions, monitoring air quality remains crucial. Aerosol optical thickness (aerosol optical depth, AOD) reflects the attenuation effect of atmospheric aerosol on light, which is an important parameter in aerosol research and plays an important role in the study of the atmosphere. Based on the CE-318 photometer data of 2015, 2016, and 2020 in Hangzhou and the MODIS satellite AOD data of 2015, 2016, and 2020, this paper first obtains the correlation between the MODIS AOD data and the ground-measured data by linear fitting. Then, the spatial and temporal distribution of the MODIS AOD data from 2012 to 2020 is analyzed. The analysis results indicate that the average correlation coefficient between the MODIS AOD data and ground-measured data is 0.77, and the average relative error is 30.53%. Thus, the MODIS AOD data can be used as an important basis for atmospheric research in Hangzhou. Based on this, the conclusions are as follows: (1) the AOD value in Hangzhou has been decreasing in recent years, from 0.43 in 2012 to 0.28 in 2020, with an average annual decrease of 0.017. (2) The AOD value in Hangzhou is large in spring and summer, and small in autumn and winter, with an average AOD value of 0.45 in spring, 0.39 in summer, 0.30 in autumn, and 0.33 in winter. (3) The AOD value in Hangzhou is large in the east and small in the west, and the AOD values in the Hangzhou urban area, Xiaoshan, and Yuhang are higher.

Keywords: AOD; validation; spatio-temporal analysis; Hangzhou

1. Introduction

The content of aerosol is important in the study of air pollution. Aerosols in the atmosphere are a system of atmospheric media and mixed solid or liquid particles with diameters ranging from 10^{-3} to 10^2 µm [1]. Although the content of aerosol in the atmosphere is very small, it significantly affects the weather and climate system [2,3], and has a great impact on climate forcing, visibility, and human health. Therefore, the study of aerosols has become a hotspot in atmospheric science research.

Atmospheric aerosols have obvious climate effects, which can affect the radiation expenditure of the earth's gas system through direct, semi-direct, and indirect effects, and are one of the uncertain factors affecting global climate change. Aerosol optical depth (AOD) measures the integration effect of aerosol extinction along a vertical path, which can reflect the attenuation effect of atmospheric aerosol on the light. It is an important parameter in aerosol research and is a good reflection of climate changes. Shao et al. [4] found that multiple meteorological factors affect each other and have a stronger influence on the change in AOD. Among them, air temperature has the strongest explanatory force on

AOD and is the dominant interaction factor. Wang et al. [5] found that AOD in Changzhou had obvious seasonal changes, with the highest in summer and the lowest in winter, and analyzed the variation characteristics of AOD in Changzhou from temporal and spatial perspectives. Zhang et al. [6] analyzed the urban heat island strength through AOD. AOD monitoring methods mainly include ground monitoring and remote sensing. The ground monitoring method refers to the establishment of observation facilities on the ground to monitor the aerosol optical depth (AOD) in the atmosphere. On the other hand, remote sensing involve instruments and equipment deployed on high-altitude platforms such as aircraft or satellites to detect AOD. Based on this standard, the following methods can be included in each category: ground-based monitoring methods—optical sensors, photometers, atmospheric radiative transfer modes; and remote sensing methods— remote sensing technology, LiDAR, optical projection technology. Compared with aerial monitoring methods, ground monitoring methods can obtain higher precision and more continuous data. However, the conventional ground monitoring methods require a lot of human power and material resources, so it is difficult to obtain large-area and long-term data. Furthermore, it is challenging to set up AOD monitoring stations in regions with a poor economy and environmental conditions. The method of AOD inversion by satellite remote sensing has the advantages of wide coverage, convenient and fast information acquisition, and has a broad development prospects.

Since the mid-1970s, the question of how to use satellite remote-sensing data to retrieve atmospheric aerosol parameters has attracted much attention worldwide. At first, the research mainly focused on the inversion of ocean surface aerosols. In 1975, Griggs put forward the theoretical basis for satellite remote sensing of aerosol optical thickness and used the first channel of AVHRR of NOAA (0.63 μm) to study the aerosol optical thickness over the ocean [7]. Gordon first considered the influence of aerosol on ocean color remote sensing [8].

In 1978, the research conducted by Tanre et al. made people realize the importance and feasibility of removing the fuzzy effect of the atmosphere, especially aerosol, in terrestrial remote sensing. After this, the remote-sensing research of terrestrial aerosol started [9], and the remote-sensing algorithms of terrestrial aerosol were developed rapidly. Scientists proposed the land–ocean comparison method [10], structure–function method [11], dark image element method [12], and thermal infrared contrast method [13]. Later, these algorithms were further developed. During this period, an algorithm for retrieving global aerosol optical thickness from EOS-MODIS was developed [14].

In 1999, the successful launch of the TERRA satellite equipped with the MODIS sensor marked a new stage of aerosol inversion by land remote sensing. Researchers began to carry out a great deal of work on MODIS aerosol retrieval. In this process, it was found that MODIS data can effectively promote air pollution monitoring and improve the monitoring of ground-based measurement data for predicting air quality. To give MODIS products better practical values, researchers conducted a lot of verification work on ground-based observation data. For example, the AERONET (Aerosol Robotic Network) program is a federation of ground-based remote sensing aerosol networks established by NASA and PHOTONS. Remer et al. [15] used the observations of AERONET to verify the validity of aerosol optical thickness at 660 nm and 870 nm of global ocean MODIS data on the global scale, and they found that the offset is small and has a good correlation. The verification of marine MODIS AOD by Levy et al. [16] indicated that MODIS AOD at 0.66 μm is closest to the ground data, with AOD values of 0.47 μm and 0.55 μm being higher, and AOD values at 0.87 μm being lower. The verification of MODIS AOD in Beijing and Hong Kong by Li et al. [17] showed that the difference between the MODIS inversion results and ground data in Beijing is larger than that in Hong Kong, and this is mainly caused by the lack of vegetation cover in the former. In Asian countries, Nichol et al. [18] evaluated the products with MODIS C6 AOD at a resolution of 3 km by AERONET data. It was found that the retrieval accuracy is generally not high, and the reliability of the products is lower than that of MODIS C6 AOD products at a resolution of 10 km. Belle et al. [19] studied the

coverage and accuracy of MODIS C6 AOD products in atmospheric air-quality research in the United States, and they found that the accuracy in the eastern part of the United States is better than that in California and western regions.

In addition to verifying the feasibility of the product, researchers also analyzed the AOD changes in specific areas based on the product. Zhai et al. [20] analyzed the temporal and spatial variation characteristics of AOD in the Yangtze River Delta region from 2000 to 2012 by using MODIS AOD products. It was found that the AOD in spring and summer is higher than that in autumn and winter. Furthermore, the spatial distribution of aerosol optical thickness is closely related to topography and population density. In general, a high AOD is distributed in low-lying plains, and a low AOD is distributed in mountainous areas.

To improve the actual availability of MODIS AOD products, researchers compared the AOD products obtained by different algorithms and developed new algorithms to improve the accuracy of MODIS AOD products.

Tao et al. [21] verified the AOD products obtained by the MODIS Collection 6 (C6) aerosol retrievals Deep Blue (DB) algorithm and Dark Target (DT) algorithm over China. They found that the two algorithms are quite different, and the AOD products obtained by the two algorithms in different regions have different characteristics. Thus, it is necessary to judge the MODIS AOD products according to the actual situation. Wei et al. [22] proposed a new aerosol inversion algorithm based on the priori LSR (Land Surface Reflectance) database (High-resolution Aerosol Retrieval algorithm with a priori LSR database Support, HARLS). Meanwhile, they compared the product obtained by this algorithm with the MODIS AOD products obtained by the DB algorithm and DT algorithm and conducted a verification in the Beijing–Tianjin–Hebei region of China. It was found that the HARLS in this region has a higher inversion accuracy and reliability and small deviation, which is generally better than the conventional AOD products in the Beijing–Tianjin–Hebei region. Bilal et al. [23] merged the AOD products obtained by the DB algorithm and DT algorithm in the MODIS C6 product set to form a new DTB3K AOD product, and they verified the new product in Europe. It was found that the product has good accuracy and strong applicability.

Researchers compared the products of different versions of MODIS AOD and the AOD products obtained by different satellites, and the results indicated that the accuracy of MODIS AOD is higher, and the accuracy is constantly improved with the update of the version. Bilal et al. [24] verified the authenticity of the DT algorithm and DB algorithm of MODIS C6 and C6.1 products on various vegetation surfaces around the world through the AERONET aerosol optical thickness data from 2004 to 2014. The verification results showed that the performance of C6.1 products is significantly better than that of C6 products, but it still needs to be improved in some areas. Almazroui [25] compared the AOD product of Collection-51 (C-51) and Collection-06 (C-06) 550 nm obtained by the MODIS DB algorithm with the AOD obtained by the ground aerosol robotic network (AERONET). It was found that the C-06 product is better than the C-51 product in the area of Sun Village in Saudi Arabia, but the overall effect is not ideal. Mangla et al. [26] compared the accuracy of MISR, MODIS, and OMI satellite products in India, and they found that MODIS has the highest accuracy, followed by MISR and OMI. Furthermore, the MODIS AOD product has wider applications in India.

Hangzhou is the capital of Zhejiang Province, and it is a new first-tier city in China and the host city of the G20 summit in 2016. More attention should be paid to the quality of the atmospheric environment in this city during its continued economic development. At present, the monitoring of AOD in Hangzhou is mainly based on fixed-point observation on the ground, and this monitoring method has limitations, as mentioned above. To better study the situation of AOD in Hangzhou, this study first tests the authenticity of the MODIS AOD products in Hangzhou and then takes years and seasons as units to study the changes in AOD in Hangzhou from 2012 to 2018. Finally, this paper studies the spatial distribution of AOD in Hangzhou.

2. Data and Methods

2.1. General Situation of the Study Area

Hangzhou is in the southeast coastal area of China, and it is the capital of Zhejiang Province. It is located in the Yangtze River Delta economic belt, and its economic level is at the forefront of the country. The climate is subtropical monsoon, where summer is hot and rainy, and winter is cold and dry. The eastern part of Hangzhou belongs to the northern Zhejiang plain. In this region, the terrain is low and flat, with a dense river network. The west of Hangzhou belongs to the hilly area of western Zhejiang, with a high altitude and many mountains. The topography of Hangzhou is mainly plain and hilly and mountainous, and the overall topography is relatively flat.

According to the administrative division of Hangzhou in 2018 [27], the study area consists of eight districts and counties: Hangzhou City, Lin'an, Xiaoshan, Yuhang, Fuyang, Tonglu, Chun'an, and Jiande, as shown in Figure 1.
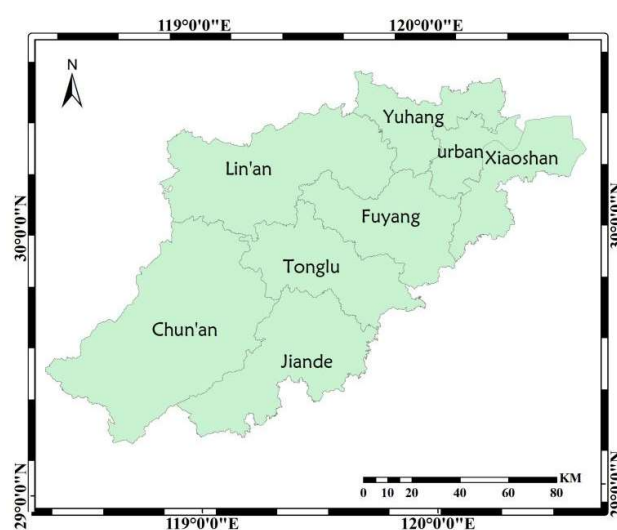

Figure 1. Administrative division map of Hangzhou (2018) ("urban" refers to the main urban area of Hangzhou City).

2.2. Data Source

The data used in this study are the AOD data of Hangzhou city from 2012 to 2020 and the Hangzhou CE-318 solar photometer data from 2015, 2016, and 2020.

The AOD data from 2012 to 2020 is a MODIS/Terra atmospheric level-2 data product with a resolution of 3 km (MOD04_3K). The MOD04 products provide aerosol optical thickness retrieved from the daily satellite transit data. The product data were generated by the Dark Target (DT) method. The reflectance of dense vegetation, wet soil and water covering areas on land is very low in the visible band, which is called dark pixel in remote sensing images. On land, dark pixels in clear skies, and in cloudless weather, the reflectance observed by satellites increases monotonously with the optical thickness of atmospheric aerosol. The algorithm for retrieving atmospheric aerosol optical thickness based on this relationship is called the Dark Target (DT) method. With improvements, the product can provide dynamic and rich surface optical images, and it has been widely used all over the world. The data were obtained from the NASA official website (https://earthdata.nasa.gov/, accessed on 31 December 2020), and the valid AOD data of Hangzhou from 1 January 2012 to 31 December 2020 were selected.

The CE-318 solar photometer data in 2015, 2016, and 2020 are from the Hangzhou Meteorological Bureau [27]. The CE-318 automatic tracking scanning solar photometer is produced by the CIMEL company in France, and the center wavelengths of the filter is 340, 380, 440, 500, 670, 870, 936, 1020, and 1640 nm. The bandwidth of each band is 10 nm. The measured value of direct solar radiation can be used, and the AOD can be calculated by using a unified inversion algorithm. In this study, the Hangzhou Meteorological Bureau

provided the measured AOD data of eight observation stations (Hangzhou City, Lin'an District, Xiaoshan District, Yuhang District, Fuyang District, Tonglu County, Chun'an County, and Jiande City) in 2015, 2016, and 2020. The longitude and latitude of each observation station are shown in Table 1, and the geographical distribution of the stations is shown in Figure 2.

Table 1. The longitude and latitude of the ground observation station in Hangzhou.

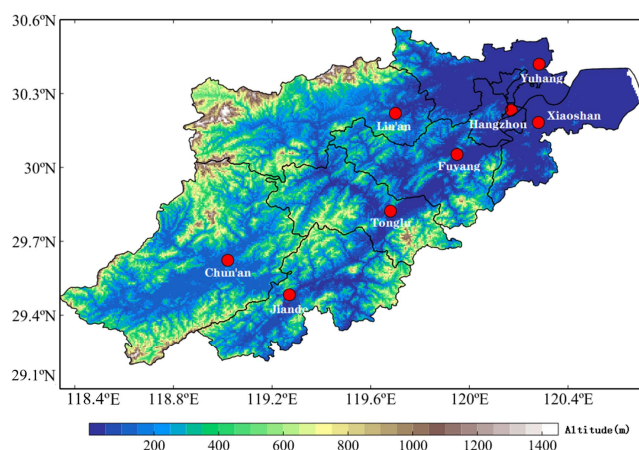| District/County	Latitude	Longitude
Hangzhou urban area	30°14′ N	120°10′ E
Lin'an District	30°13′ N	119°42′ E
Xiaoshan District	30°11′ N	120°17′ E
Yuhang District	30°25′ N	120°17′ E
Fuyang district	30°03′ N	119°57′ E
Tonglu County	29°49′ N	119°41′ E
Chun'an County	29°37′ N	119°01′ E
Jiande City	29°29′ N	119°16′ E

Figure 2. The location of the ground observation stations in Hangzhou.

2.3. Research Methods

In this study, the MODIS/Terra Atmospheric level-2 data product at 550 nm with a resolution of 3 km (MOD04_3K) was used as the MODIS AOD data, and the AOD observation product with the highest quality mark (Quality Flag = 3) was selected [28]. The data extraction method matched photometer data and satellite AOD data by determining the time window and space range. The selection of the time window was based on the transit time of the satellite, and the AOD data of the photometer of the monitoring station were selected and averaged at a time interval of 30 min. The selection of the spatial range took the ground monitoring station as the center and selected the MODIS AOD data within 3 × 3 pixels around the center. If more than 4 pixels out of 9 pixels had a value, then the average value was taken as the AOD value of the point; if the number of pixels with a value was less than 4, then the value of the point was discarded [18]. Finally, the matching photometer–MODIS AOD data set was formed.

After the photometer data and MODIS data were matched in time and space, a linear fitting analysis was conducted between them. The fitting results were evaluated by the parameters of linear regression, such as slope *a*, intercept *b*, correlation coefficient *R*, and mean relative error (MRE).

Because the photometer does not have 550 nm band data, based on the major optical parameter for measuring the aerosol particle size [29], the "Angstrom exponent", this study

interpolates the AOD value (λ = 500 nm) obtained by the photometer into 550 nm [18], as shown in Formula (1):

$$\text{AOD}_{550\text{nm}} = \text{AOD}_{500\text{nm}}(550/500)^{-440-670\alpha} \tag{1}$$

There is a certain relationship between the AOD value and wavelength, as shown in Formula (2) [30]:

$$\tau(\lambda) = k\lambda^{-\alpha} \tag{2}$$

where $\tau(\lambda)$ is the AOD value of the corresponding band, k is the Angstrom turbidity coefficient that can represent the thickness of aerosol in the atmosphere, and α is the Angstrom wavelength index. By substituting different wavelength values and the corresponding AOD values into Formula (3) and taking logarithms, the Angstrom wavelength index α [31] can be calculated:

$$\alpha = \frac{-ln\left(\tau_{\lambda 1}/\tau_{\lambda 2}\right)}{ln(\lambda 1/\lambda 2)} \tag{3}$$

In Formula (3), λ is the band, and τ_λ is the AOD value of the corresponding band. In this paper, the bands of 440 nm and 670 nm ($\lambda 1 = 440$ nm, $\lambda 2 = 670$ nm) and their corresponding ground-measured AOD values are selected as the basic data for calculating α.

3. Results and Discussion

3.1. Analysis of the Authenticity of the MODIS AOD Data in Hangzhou

In this study, the obvious outliers in the MODIS AOD data obtained by spatio-temporal matching and the AOD data measured by the corresponding ground photometer were removed by standard deviation, and the rest of the data were linearly fitted. After removing the abnormal values, a total of 49 pairs of normal data sets in 2015, 56 pairs of normal data sets in 2016, 74 pairs of normal data sets in 2020, and 179 pairs of normal data sets in three years were obtained.

Figure 3, Figure 4, and Figure 5, respectively, show the comparison of 2015, 2016, and 2020 MODIS AOD data with the ground photometer-measured AOD data. Figure 6 shows the comparison of all MODIS AOD data with the ground photometer-measured AOD data in three years. The correlation coefficient obtained by linear fitting of the 2015 MODIS AOD data is 0.77, and the average relative error is 30.64%; the correlation coefficient obtained by linear fitting of the 2016 MODIS AOD data is 0.75, and the average relative error is 30.57%; the correlation coefficient obtained by linear fitting of the MODIS AOD data in 2020 is 0.69, and the average relative error is 30.08%. After summarizing the three-year MODIS AOD data, the correlation coefficient R of all the data is 0.77, and the average relative error MRE is 30.53%. It can be seen from the overall fitting results that there is a high correlation coefficient between the MODIS AOD data and the ground photometer-measured AOD data. These comparison results prove that the accuracy of the MODIS AOD data in Hangzhou is high, and the data can be used for observing the AOD values in this area.
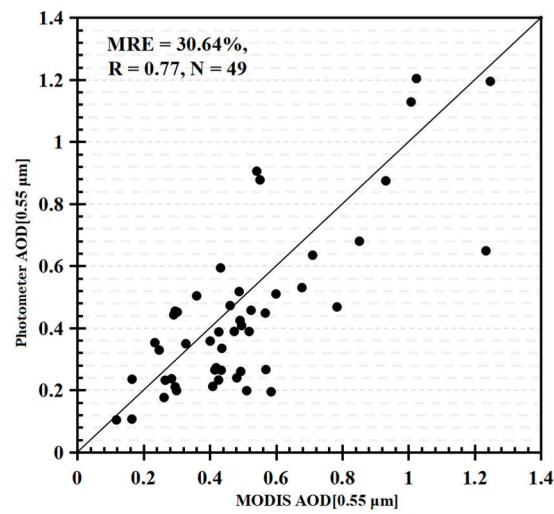
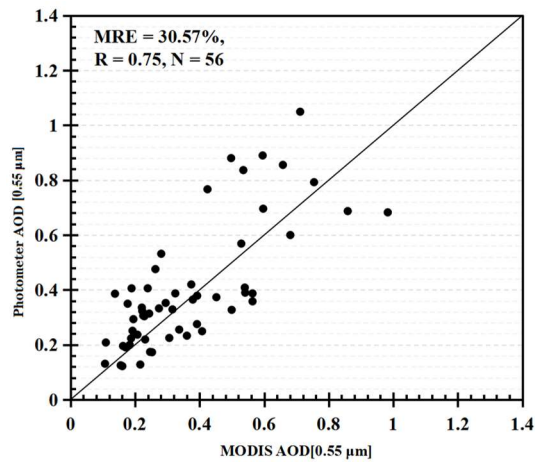**Figure 3.** The comparison between the MODIS AOD data and the ground photometer AOD data in 2015 ($p < 0.05$).

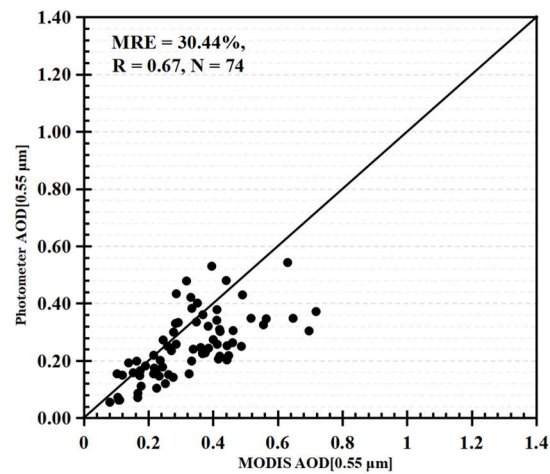**Figure 4.** The comparison between the MODIS AOD data and the ground photometer AOD data in 2016 ($p < 0.05$).

Figure 5. The comparison between the MODIS AOD data and the ground photometer AOD data in 2020 ($p < 0.05$).
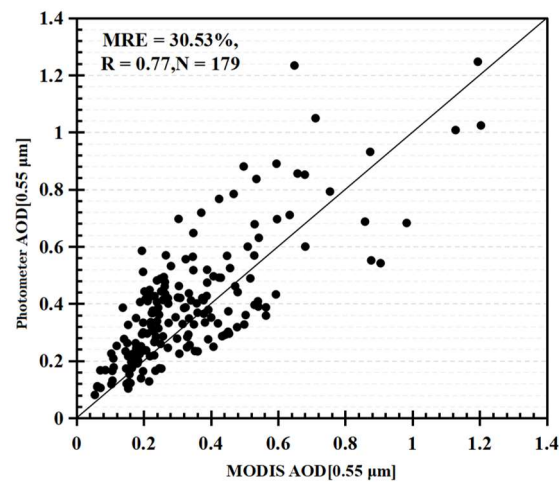
Figure 6. The comparison of the MODIS AOD data and the ground photometer AOD data in three years ($p < 0.05$).

3.2. *Time Distribution Characteristics of AOD in Hangzhou from 2012 to 2020*

3.2.1. Annual Variation Characteristics

Based on the average value of the annual AOD data from 2012 to 2020, the change in the average AOD value in Hangzhou in the past nine years is obtained. It can be seen from Figure 7 that although the AOD value in Hangzhou slightly increased in 2013, 2017, and 2019, it shows an overall downward trend, indicating that the air quality of Hangzhou has been improving in recent years. Hangzhou began to implement the bill on comprehensive air pollution control in 2002 to protect the atmospheric environment in stages. In 2014, Hangzhou began to implement an action plan for air pollution prevention and control. The proposal of relevant policies provides a good basis for atmospheric governance in Hangzhou, combined with an increasing awareness of atmospheric protection of the citizens, so the atmospheric environmental quality of Hangzhou has been continuously improved in recent years. The improvement of air quality is also closely related to urban activities. The G20 summit was held in Hangzhou in 2016, and various measures were taken to prevent and control air pollution, such as expanding the scope of no-burning zones for highly polluting fuels, strengthening comprehensive pollution control in key industries, and promoting clean-production audits and technological transformations in five key industries. Attributed to this, the air quality has been significantly improved.
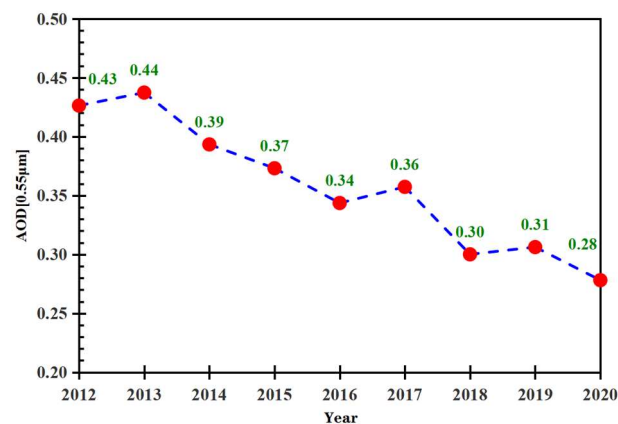

Figure 7. The change in annual AOD values in Hangzhou from 2012 to 2018.

The number of days with AOD values greater than 0.5 was analyzed, and its distribution from 2012 to 2020 was obtained and shown in Figure 8. It can be seen that from 2012 to 2020, the annual days with AOD values greater than 0.5 show an overall downward

trend. Specifically, from 92 days in 2012 to 36 days in 2020, there is a decrease of 56 days. However, in terms of annual changes, the number of days with AOD values greater than 0.5 increased in 2013, 2017, and 2019. Especially in 2013, there is an increase of 68 days. This trend is the same as that in Figure 7.
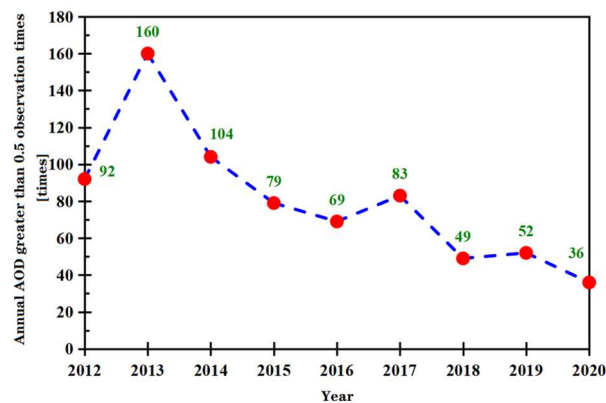

Figure 8. The distribution of times with AOD greater than 0.5.

According to the measured atmospheric data provided by the Hangzhou Meteorological Bureau, Figures 9 and 10 are obtained. It can be seen from Figure 9 that the annual haze days in Hangzhou from 2012 to 2020 can be divided into three stages. The first stage is from 2012 to 2014, during which there is almost no significant decrease or increase in the number of annual haze days in Hangzhou, and the annual change is less than 10 days. The second stage is from 2014 to 2018, during which the number of annual haze days in Hangzhou shows a significant downward trend, and the decline in 2016 is the most obvious, i.e., 35 days. The third stage is from 2018 to 2020, during which the number of annual haze days in Hangzhou first increased by 42 days in 2019 and then decreased in 2020. Generally, during the nine years from 2012 to 2020, the number of annual haze days in Hangzhou first fluctuates slightly, then begin to decrease obviously, and finally increases to a certain extent, indicating that the air quality in Hangzhou began to improve continuously in 2014 and began to decrease in 2019.
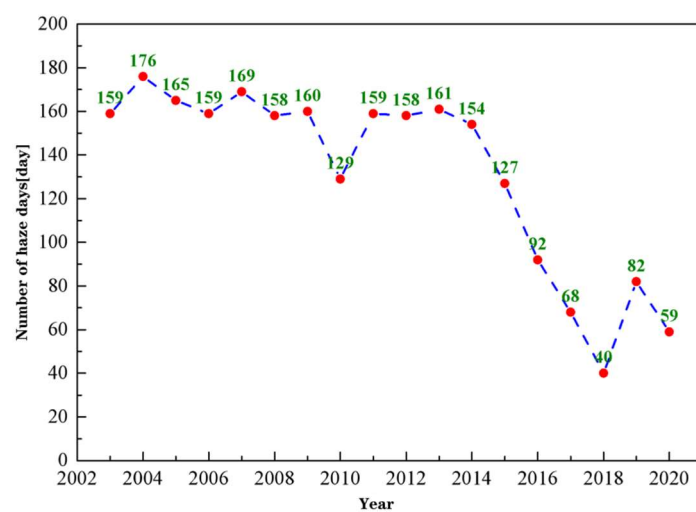

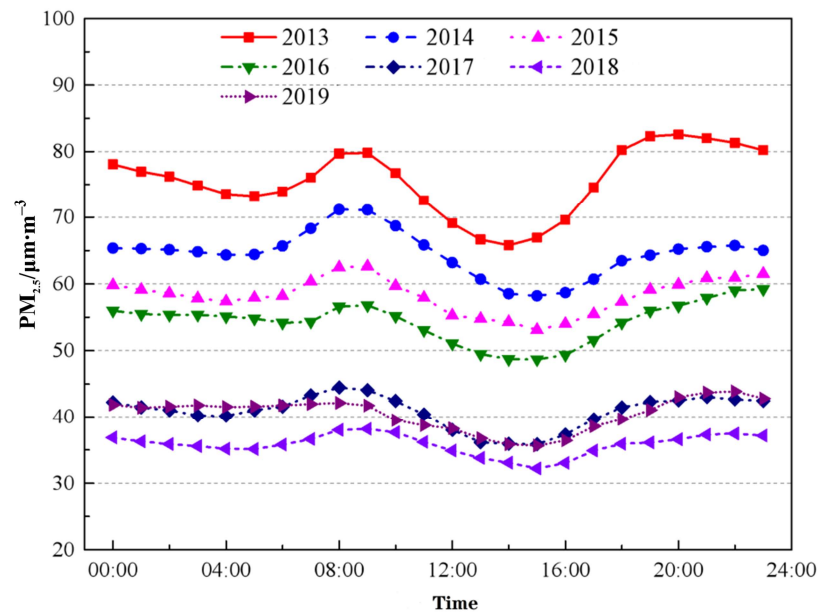**Figure 9.** The number of haze days in Hangzhou from 2003 to 2019.

Figure 10. The change in PM2.5 in Hangzhou from 2013 to 2019.

As shown in Figure 10, the change in daily PM2.5 in Hangzhou from 2013 to 2019 indicates that the daily PM2.5 in Hangzhou has an obvious variation trend, with a larger value at 8 o'clock and 20:00 and a smaller value at 14:00. From the change over the years, the average annual PM2.5 in Hangzhou shows a steady downward trend from 2013 to 2018, and the annual PM2.5 increased in 2019. This indicates that the air quality of Hangzhou improved continuously from 2012 to 2018 but decreased in 2019.

The data of annual haze days and annual PM2.5 in Hangzhou reflect the continuous improvement in air quality in Hangzhou in recent years. This changing trend is similar to that of the average annual AOD and the distribution of observation days with AOD values greater than 0.5. Therefore, the MODIS AOD data are authentic and is a good reflection of the air-quality changes in Hangzhou.

3.2.2. Seasonal Variation Characteristics

The AOD data of Hangzhou from 2012 to 2020 are divided into seasons according to the division of spring from March to May, summer from June to August, autumn from September to November, and winter from December to February. Then, the seasonal average AOD variation in Hangzhou from 2012 to 2020 is obtained and shown in Figure 11. In terms of the seasonal distribution, the AOD value in Hangzhou is relatively low in autumn and winter and high in spring and summer, with the lowest in autumn and the highest in spring. The causes of this result are analyzed as follows. In spring, Hangzhou is easily affected by the dust storms in the north or local pollution sources [32]. Combined with the fact that the temperature begins to warm up in spring, the atmosphere is relatively stable, which is favorable for the long-term retention of atmospheric aerosol particles, so the AOD value in spring is higher. Hangzhou has a high temperature and is rainy in summer, and the high temperature and high humidity conditions will promote the formation of aerosols, leading to urban aerosol accumulation [33], so the AOD value in summer is higher. In addition, the unstable subtropical monsoon climate results in a large dispersion of AOD values in spring and summer. The temperature drops in autumn, the wind is strong, the atmospheric condition is unstable, and it is difficult for the aerosol particles to remain for a long time. In this case, the AOD value is low in autumn. The northwest wind prevails in winter, the wind is strong, the atmospheric condition is unstable, but the air is dry. Because of this, the surface is bare, and there is much dust in winter, so the AOD value in winter is higher than that in autumn.
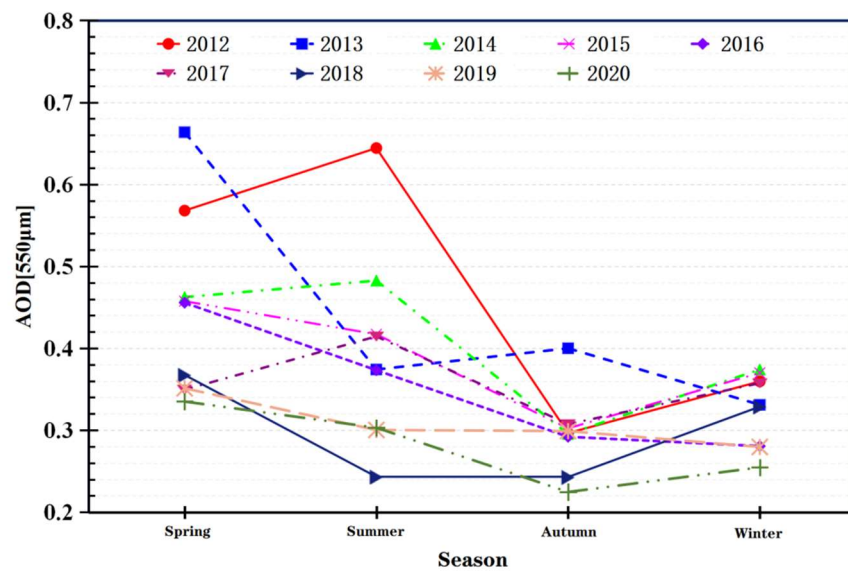
Figure 11. The change in AOD in Hangzhou from 2012 to 2020.

The specific situation of each year indicates that the AOD value of each season is quite different from the overall situation. For example, in 2012, 2014, and 2017, the AOD value in summer is higher than that in spring, and the AOD value in autumn of 2013 is higher than that in winter. The atmospheric environmental conditions are different in different years and seasons, so the seasonal distribution of AOD values is also different.

3.3. Spatial Distribution Characteristics of AOD in Hangzhou from 2012 to 2020

The average annual AOD values of Hangzhou, Lin'an, Xiaoshan, Yuhang, Fuyang, Tonglu, Chun'an, and Jiande from 2012 to 2020 are compared, and the AOD distribution from 2012 to 2020 is obtained and shown in Figure 12. It can be seen that the AOD value in Hangzhou is higher in 2013 and begins to decline in 2013. For specific districts and counties, the AOD value in Hangzhou is mainly large in the east and small in the west. Among all the regions, the AOD values of Hangzhou, Xiaoshan, and Yuhang in the northeast are the highest. These three regions are located in the Hangjiahu Plain with large population density and developed industry. In addition, the hills and mountains in the west and south reduce the atmospheric loss and cause atmospheric aerosol particles to gather in this region, so the AOD value of this region is larger, and the atmospheric quality is poor. By contrast, there are many mountains in the west and north with less population, so the air quality is relatively good.
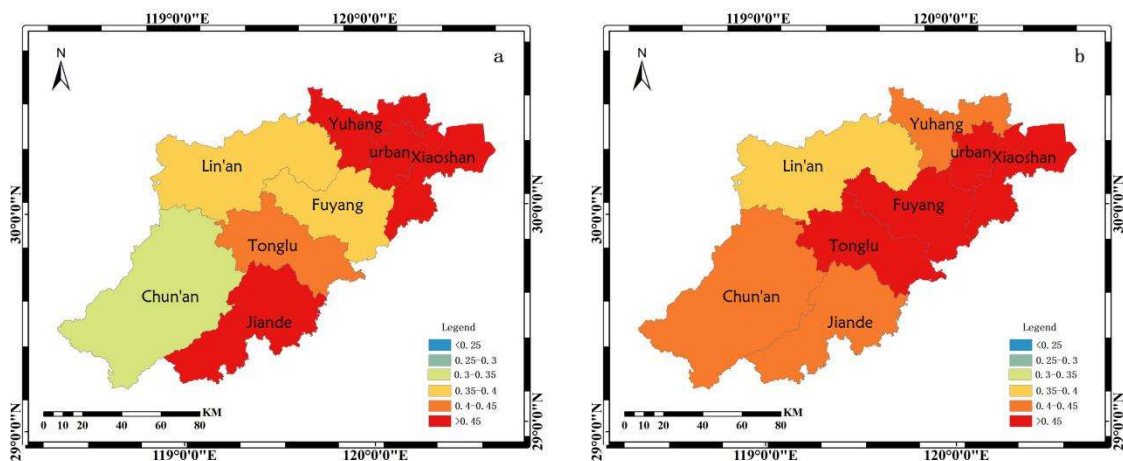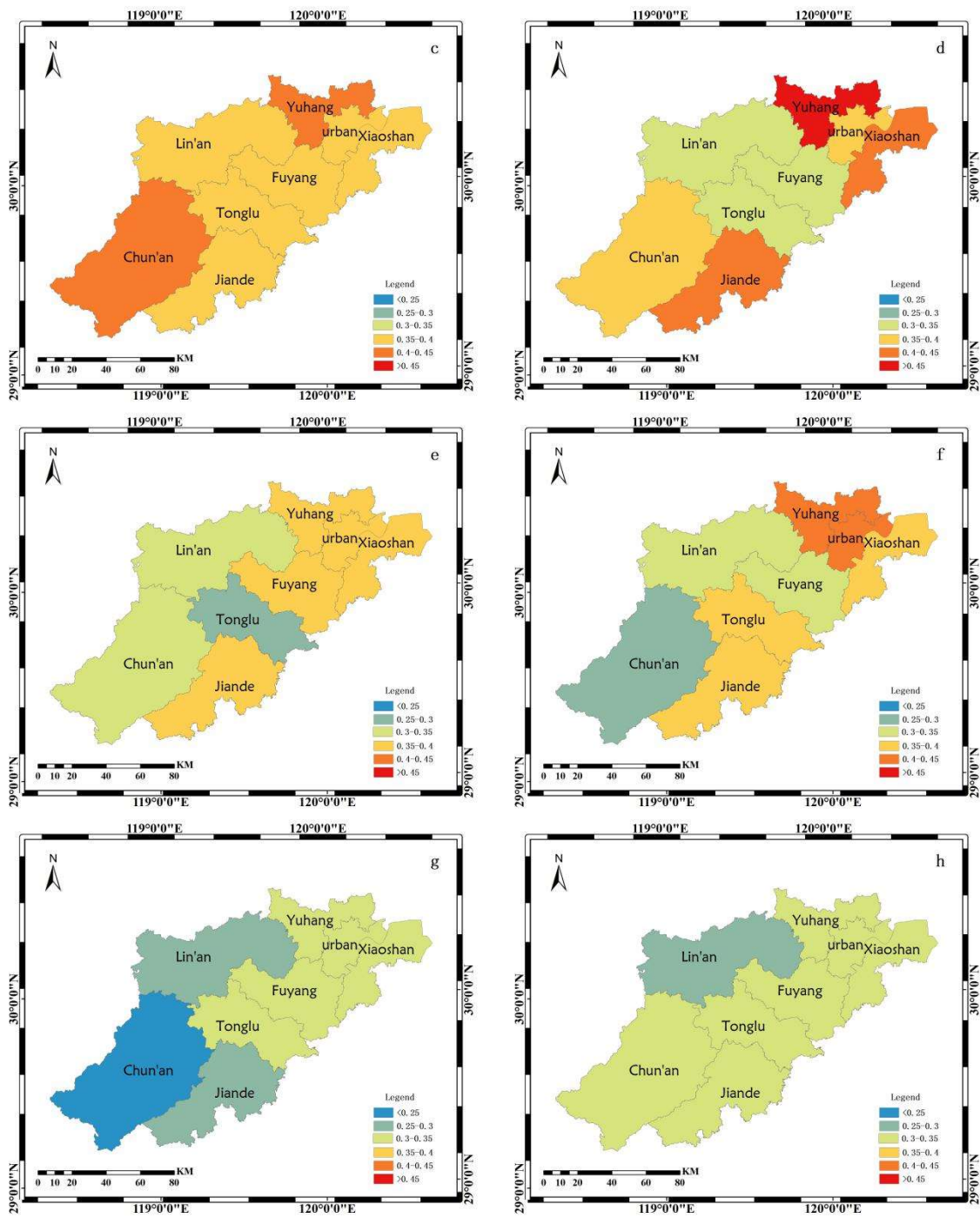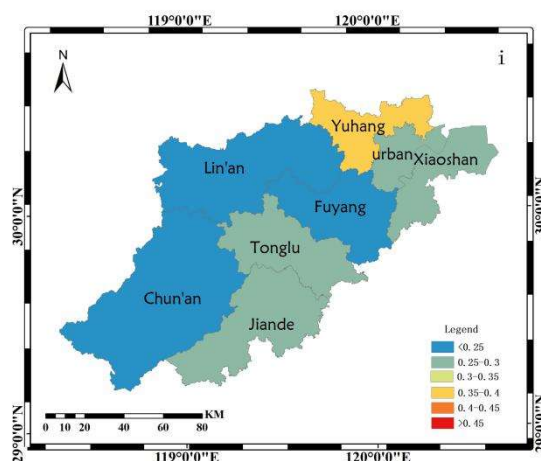

Figure 12. *Cont.*

Figure 12. *Cont*.

Figure 12. The AOD distribution of Hangzhou counties and districts from 2012 to 2020: (**a**) 2012, (**b**) 2013, (**c**) 2014, (**d**) 2015, (**e**) 2016, (**f**) 2017, (**g**) 2018, (**h**) 2019, and (**i**) 2020.

4. Conclusions

In this paper, by analyzing the photometer data obtained by the ground monitoring stations in Hangzhou in 2015, 2016, and 2020 and the MODIS AOD data from 2012 to 2020, the following conclusions are drawn:

(1) The photometer data obtained by the ground monitoring stations in Hangzhou in 2015, 2016, and 2020 are matched with the MODIS AOD data of Hangzhou in 2015, 2016, and 2020. The correlation between the two types of data is obtained by linear fitting, and the correlation coefficients in 2015, 2016, 2020, and three years are, respectively, 0.77, 0.75, 0.67, and 0.77. The average relative error is 30.64% for the data in 2015, 30.57% for the data in 2016, and 30.44% for the data in 2020, and the average relative error of all data in three years is 30.53%. Therefore, there is a good correlation between the MODIS AOD data and the ground-measured AOD data in Hangzhou. The MODIS AOD data can be used as an important basis for studying the AOD of Hangzhou.

(2) Hangzhou experienced three stages of annual haze days from 2012 to 2020. The first stage was from 2012 to 2014, with almost no significant change in annual haze days. The second stage is from 2014 to 2018, with a significant downward trend in the number of haze days per year. The third stage is from 2018 to 2020, during which the number of annual haze days first decreased in 2019. The daily value of PM2.5 shows a clear trend of change, with significant changes at 8:00 a.m. and 8:00 p.m., and small changes at 2:00 p.m.

(3) Based on the analysis of the annual AOD data of Hangzhou from 2012 to 2020, the AOD value in Hangzhou shows a downward trend in the last nine years, indicating that the air quality of Hangzhou has been improving. This observation is consistent with the measured air-quality distribution map.

(4) The AOD data from 2012 to 2020 are divided into seasons following the division of spring from March to May, summer from June to August, autumn from September to November, and winter from December to February. It can be seen that the annual AOD seasonal distribution is different, but on the whole, the AOD values in autumn and winter are lower, those in spring and summer are higher, and those in autumn are the lowest.

(5) The average annual AOD values of Hangzhou, Lin'an, Xiaoshan, Yuhang, Fuyang, Tonglu, Chun'an, and Jiande from 2012 to 2020 are compared. It can be observed that the AOD value in Hangzhou is low in the west and high in the east. Among the regions, the AOD values of Hangzhou, Xiaoshan, and Yuhang are higher.

Author Contributions: Conceptualization, X.Y. and B.W.; Data curation, Y.X., J.H. and M.C.; Investigation, B.Q. and Z.Y.; Methodology, X.Y. and B.W.; Writing—original draft, X.Y. and M.C.; Writing—review & editing, Z.Y. and B.W. All authors have read and agreed to the published version of the manuscript.

Data Availability Statement: Enquiries regarding in situ data availability should be directed to the authors. The MOD04_3K AOD data that support the findings of this study are openly available in Giovanni at https://giovanni.gsfc.nasa.gov/giovanni/, accessed on 31 December 2020.

References

1. Fu, B.; Xie, Y.; Cui, X. Anyang City Atmospheric Aerosol Laser Radar in Autumn and Winter Monitoring Case. *Green Sci. Technol.* **2022**, *24*. [CrossRef]
2. Charlson, R.J.; Schwartz, S.E.; Hales, J.M.; Cess, R.D.; Coakley, J.A., Jr.; Hansen, J.E.; Hofmann, D.J. Climate forcing by anthropogenic aerosols. *Science* **1992**, *255*, 423–430. [CrossRef] [PubMed]
3. Guo, J.; Deng, M.; Lee, S.S.; Wang, F.; Li, Z.; Zhai, P.; Liu, H.; Lv, W.; Yao, W.; Li, X. Delaying precipitation and lightning by air pollution over the Pearl River Delta. Part I: Observational analyses. *J. Geophys. Res. Atmos.* **2016**, *121*, 6472–6488. [CrossRef]
4. Wen, S.; Liu, H.; Gao, Y.; Qian, Y. Spatiotemporal evolution and meteorological interpretation of aerosol optical thickness in Beijing, Tianjin and Hebei. *Sci. Technol. Eng.* **2022**, *22*, 13569–13577.
5. Wang, Z.; Li, L.; Yu, Y.; Yang, W.; Zhou, W.; Ye, X.; Zhao, Y. Study on the spatial and temporal change characteristics of MODIS aerosol optical thickness in Changzhou from 2000 to 2019. *Environ. Monit. China* **2023**, *39*, 223–230.
6. Zhang, X.; Wang, X.; Zheng, Y.; Cui, S.; Yang, X.; Jiang, Z. Effect of aerosol optical thickness and impervious surface coverage on urban heat island strength—Take Guanzhong area as an example. *J. Ecol.* **2021**, *41*, 8965–8976.
7. Griggs, M. Measurements of atmospheric optical thickness over water using ERTS-1 data. *J. Air Pollut. Control Assoc.* **1975**, *25*, 622–626. [CrossRef]
8. Gordon, H.R. Removal of atmospheric effects from satellite imagery of the oceans. *Appl. Opt.* **1978**, *17*, 1631–1636. [CrossRef]
9. Tanre, D.; Herman, M.; Deschamps, P.Y.; de Leffe, A. Atmospheric modeling for space measurements of ground reflectances, including bidirectional properties. *Appl. Opt.* **1979**, *18*, 3587. [CrossRef]
10. Kaufman, Y.J. Solution of the equation of radiative transfer for remote sensing over two-dimensional surface reflectivity. *J. Geophys. Res. Ocean.* **1982**, *87*, 4137–4147. [CrossRef]
11. Tanré, D.; Deschamps, P.Y.; Devaux, C.; Herman, M. Estimation of Saharan aerosol optical thickness from bluring effects in Thematic Mapper data. *J. Geophys. Res. Atmos.* **1988**, *93*, 15955–15964. [CrossRef]
12. Kaufman, Y.J.; Sendra, C. Algorithm for automatic atmospheric corrections to visible and near-IR satellite imagery. *Int. J. Remote Sens.* **1988**, *9*, 1357–1381. [CrossRef]
13. Legrand, M.; Ducroz, F. MSA to non sea-salt sulfate ratio in coastal Antarctic aerosol and surface snow. *J. Geophys. Res.* **1989**, *103*, 10991–11106. [CrossRef]
14. Kaufman, Y.J.; Tanre, D. Algorithm for Remote Sensing of Aerosol from MODIS. *MODIS Algorithm Theor. Basis Doc.* **1998**. [CrossRef]
15. Remer, L.A.; Tanre, D.; Kaufman, Y.J.; Ichoku, C.; Mattoo, S.; Levy, R.; Chu, D.A.; Holben, B.; Dubovik, O.; Smirnov, A.; et al. Validation of MODIS aerosol retrieval over ocean. *Geophys. Res. Lett.* **2002**, *29*, MOD3-1–MOD3-4. [CrossRef]
16. Levy, R.C.; Remer, L.A.; Tanré, D.; Kaufman, Y.J.; Ichoku, C.; Holben, B.N.; Livingston, J.M.; Russell, P.B.; Maring, H. Evaluation of the Moderate-Resolution Imaging Spectroradiometer(MODIS) retrievals of dust aerosol over the ocean during PRIDE. *J. Geophys. Res.* **2003**, *108*, 13. [CrossRef]
17. Li, C.; Mao, J.; Lau, K.H.A.; Chen, J.C.; Yuan, Z.; Liu, X.; Zhu, A.; Liu, G. Characteristics of distribution and seasonal variation of aerosol optical depth in eastern China with MODIS products. *Chin. Sci. Bull.* **2003**, *48*, 2488–2495.
18. Nichol, J.E.; Bilal, M. Validation of MODIS 3 km Resolution Aerosol Optical Depth Retrievals Over Asia. *Remote Sens.* **2016**, *8*, 328. [CrossRef]
19. Belle, J.H.; Liu, Y. Evaluation of Aqua MODIS Collection 6 AOD Parameters for Air Quality Research over the Continental United States. *Remote Sens.* **2016**, *8*, 815. [CrossRef]
20. Zhai, T.; Zhao, Q.; Gao, W.; Shi, R.; Xiang, W.; Huang HL, A.; Zhang, C. Analysis of spatio-temporal variability of aerosol optical depth with empirical orthogonal functions in the Changjiang River Delta, China. *Front. Earth Sci.* **2015**, *9*, 1–12. [CrossRef]
21. Tao, M.; Chen, L.; Wang, Z.; Tao, J.; Che, H.; Wang, X.; Wang, Y. Comparison and evaluation of the MODIS Collection 6 aerosol data in China. *J. Geophys. Res. Atmos.* **2015**, *120*, 6992–7005. [CrossRef]
22. Wei, J.; Sun, L. Comparison and Evaluation of Different MODIS Aerosol Optical Depth Products Over the Beijing-Tianjin-Hebei Region in China. *IEEE J. Sel. Top. Appl. Earth Obs. Remote Sens.* **2017**, *10*, 835–844. [CrossRef]
23. Bilal, M.; Qiu, Z.; Campbell, J.R.; Spak, S.N.; Shen, X.; Nazeer, M. A New MODIS C6 Dark Target and Deep Blue Merged Aerosol Product on a 3 km Spatial Grid. *Remote Sens.* **2018**, *10*, 463. [CrossRef]

24. Bilal, M.; Nazeer, M.; Qiu, Z.; Ding, X.; Wei, J. Global Validation of MODIS C6 and C6.1 Merged Aerosol Products over Diverse Vegetated Surfaces. *Remote Sens.* **2018**, *10*, 475. [CrossRef]

25. Almazroui, M. A comparison study between AOD data from MODIS deep blue collections 51 and 06 and from AERONET over Saudi Arabia. *Atmos. Res.* **2019**, *225*, 88–95. [CrossRef]

26. Mangla, R.; Indu, J.; Chakra, S.S. Inter-comparison of multi-satellites and Aeronet AOD over Indian Region. *Atmos. Res.* **2020**, *240*, 104950. [CrossRef]

27. Che, H.; Qi, B.; Zhao, H.; Xia, X.; Eck, T.F.; Goloub, P.; Dubovik, O.; Estelles, V.; Cuevas-Agulló, E.; Blarel, L.; et al. Aerosol optical properties and direct radiative forcing based on measurements from the China Aerosol Remote Sensing Network (CARSNET) in eastern China. *Atmos. Chem. Phys.* **2018**, *18*, 405–425. [CrossRef]

28. Levy, R.C.; Mattoo, S.; Munchak, L.A.; Remer, L.A.; Sayer, A.M.; Patadia, F.; Hsu, N.C. The Collection 6 MODIS aerosol products over land and ocean. *Atmos. Meas. Tech.* **2013**, *6*, 2989–3034. [CrossRef]

29. Zhang, Y. Analysis of the Microphysical Properties of Atmospheric Aerosols in Northern China. Part II: Interpretation of Result. *Curric. Educ. Eesearch* **2018**, *4*, 53–54.

30. Ångström, A. The parameters of atmospheric turbidity. *Tellus* **1964**, *16*, 64–75. [CrossRef]

31. Beegum, S.N.; Moorthy, K.K.; Babu, S.S. Aerosol microphysics over a tropical coastal station inferred from the spectral dependence of Angstrom wavelength exponent and inversion of spectral aerosol optical depths. *J. Atmos. Sol.-Terr. Phys.* **2009**, *71*, 1846–1857. [CrossRef]

32. Gong, S.L.; Zhang, X.Y.; Zhao, T.L.; Mckendry, I.G.; Jaffe, D.A.; Lu, N.M. Characterization of soil dust aerosol in China and its transport and distribution during 2001ACE-Asia: 2. Model simulation and validation. *J. Geophys. Res.* **2003**, *108*, D11202. [CrossRef]

33. Adamopoulos, A.D.; Kambezidis, H.D.; Kaskaoutis, D.G.; Giavis, G. A study on aerosols size in the atmosphere of Athens, Greece, retrieved from solar spectral measurements. *Atmos. Res.* **2007**, *86*, 194–206. [CrossRef]